

Observation of a Griffiths Phase in Paramagnetic $\text{La}_{1-x}\text{Sr}_x\text{MnO}_3$

J. Deisenhofer,¹ D. Braak,² H.-A. Krug von Nidda,¹ J. Hemberger,¹ R. M. Eremina,³ V. A. Ivanshin,⁴ A. M. Balbashov,⁵ G. Jug,⁶ A. Loidl,¹ T. Kimura,⁷ and Y. Tokura⁷

¹*EP V, Center for Electronic Correlations and Magnetism, University of Augsburg, 86135 Augsburg, Germany*

²*Theoretical Physics II, Institute for Physics, University of Augsburg, 86135 Augsburg, Germany*

³*E. K. Zavoisky Physical-Technical Institute, 420029 Kazan, Russia*

⁴*Kazan State University, 420008 Kazan, Russia*

⁵*Moscow Power Engineering Institute, 105835 Moscow, Russia*

⁶*Dipartimento di Fisica e Matematica, Università dell'Insubria, 22100 Como, Italy*

⁷*Department of Applied Physics, University of Tokyo, Tokyo 113-8656, Japan*

(Received 26 April 2005; published 12 December 2005)

We report on the discovery of a novel triangular phase regime in the system $\text{La}_{1-x}\text{Sr}_x\text{MnO}_3$ by means of electron spin resonance and magnetic susceptibility measurements. This phase is characterized by the coexistence of ferromagnetic entities within the globally paramagnetic phase far above the magnetic ordering temperature. The nature of this phase can be understood in terms of Griffiths singularities arising due to the presence of correlated quenched disorder in the orthorhombic phase.

DOI: [10.1103/PhysRevLett.95.257202](https://doi.org/10.1103/PhysRevLett.95.257202)

PACS numbers: 75.47.Gk, 71.70.Ej, 75.30.Et, 76.30.-v

Recently, the considerable influence of *quenched disorder* on the phase complexity in manganite systems and the appearance of phenomena such as colossal magnetoresistance (CMR) has been unraveled both experimentally [1,2] and theoretically [3,4]. Within the context of quenched-disorder scenarios, the existence of a Griffiths-like [5] temperature scale T_G above the magnetic ordering temperature T_C has been predicted and linked to CMR [6–8]. Moreover, the competition between charge-ordered anti-ferromagnetic (AFM) and metallic ferromagnetic (FM) phases appears to be a significant factor for the rich phase diagrams of these systems [7], and the persistence of nano-scale inhomogeneities in the paramagnetic (PM) regime has been reported early on [9].

Below T_G , the quenched disordered system is in between the completely disordered PM high-temperature regime and the magnetically ordered state. This phase regime is usually referred to as the *Griffiths phase* (GP) [10], based on Griffiths' seminal treatment of the effects of quenched randomness on the magnetization of a dilute Ising ferromagnet [5]. Griffiths showed that essential singularities would develop in a temperature region $T_C(p) < T < T_G$, where p denotes the disorder parameter, $T_C(p)$ the disorder-dependent FM ordering temperature [Fig. 4(a)], and T_G a new temperature scale corresponding to $T_C(1)$, the Curie temperature of the undiluted system with $p = 1$. Further studies showed the importance of correlated disorder in generating and enhancing the new singularities [11–13], but a systematic study of the Griffiths phenomenon in a competing 3D two-phase situation (e.g., AFM/FM) is still not available at present. The impact of Griffiths scenarios for disorder physics is evidenced by its evocation for such challenging physical problems as the non-Fermi liquid behavior in Kondo systems [14] and the properties of magnetic semiconductors [15]. To date, however, an entire

GP, i.e., a globally PM regime characterized by the temperature boundaries T_G and T_C and a well-defined disorder parameter p , has not been identified experimentally.

Here we report the discovery of an entire GP in single crystals of the paradigm system $\text{La}_{1-x}\text{Sr}_x\text{MnO}_3$ (LSMO), demonstrating the impact of quenched disorder in manganites. Using electron spin resonance (ESR) and magnetic susceptibility measurements, we clearly identify a triangular phase regime limited by the Sr concentration $x_c \sim 0.07$, the Griffiths temperature scale $T_G \sim 270$ K, and the FM transition temperature up to a maximal Sr concentration $x_{\text{max}} \sim 0.16$ [Fig. 4(c)]. Furthermore, we propose that the appearance of Griffiths-phase regimes can be expected for many other manganite systems and mapped out by ESR, which is a local magnetic probe and particularly sensitive in the PM regime.

ESR measurements were performed with a Bruker spectrometer at 9.4 and 34 GHz. Susceptibilities were measured with a SQUID magnetometer (Quantum Design). Details on the experimental setup and crystal growth have been published elsewhere [16–18].

In Fig. 1, we show ESR spectra in $\text{La}_{1-x}\text{Sr}_x\text{MnO}_3$ in the PM regime above $T_C = 180$ K. The spectra not only consist of a PM signal due to the majority of Mn^{3+} and Mn^{4+} spins [17] but also exhibit an intriguing FM resonance (FMR) signal at lower resonance fields. A rough estimate obtained by comparing the FMR and PM signals shows that the fraction of spins contributing to the FMR is $\leq 1\%$. The PM resonance signal and its anisotropy in the orbitally ordered phase have been analyzed in detail previously [18–20]. Here the focus is on the FMR signal, which emerges from the signal of the PM $\text{Mn}^{3+}/\text{Mn}^{4+}$ background ($g = 2$) at $T \approx 260$ K, far above $T_C = 180$ K [21], and then shifts towards lower resonance fields, indicating an increase of the local magnetic fields in the sample. This shift

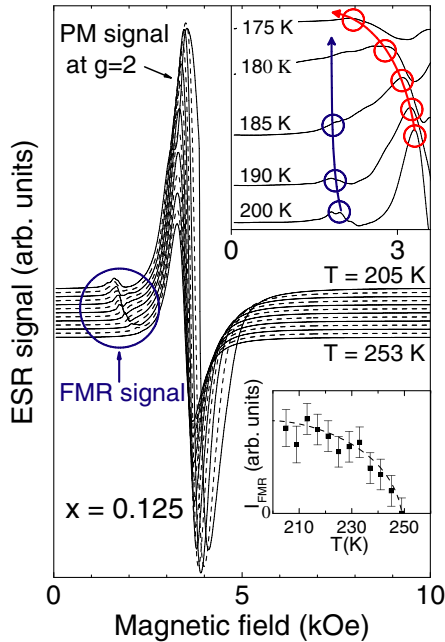


FIG. 1 (color online). ESR spectra for $x = 0.125$ for $205 \leq T \leq 253$ K with the magnetic field applied within the easy ac plane. Upper inset: Evolution of the spectra towards T_C . Lower inset: T dependence of the FMR intensity. Lines are to guide the eye.

corresponds to the T dependence of the FM magnetization [22]. Concomitantly, the intensity of the FMR (estimated via its peak-to-peak linewidth ΔH_{pp} and its amplitude A as $\Delta H_{pp}^2 \cdot A$) first clearly increases and then saturates with decreasing temperatures, as shown in the lower inset in Fig. 1. This behavior excludes a superparamagnetic origin of the signal, which would result in a T dependence according to the Langevin function [for temperatures under consideration, a Curie-Weiss (CW)-like increase] instead of a saturation.

On approaching T_C , the PM line broadens, shifts to lower resonance fields, and finally merges with the FMR (upper inset in Fig. 1). Moreover, the FMR signal exhibits a pronounced easy-plane anisotropy with respect to the ac plane ($Pnma$) of FM superexchange coupling, which is shown in Fig. 2 for a sample with $x = 0.1$ at 230 K. The lack of data at about 3.3 and 12 kOe is due to the fact that the FMR signal cannot be resolved anymore when passing through the PM signal at $g = 2$. Fitting the angular dependence of the resonance field measured at 9.4 and 34 GHz by taking into account first and second order anisotropy fields H_{A_1} and H_{A_2} [22] results in $H_{A_1} = -2.4$ kOe and $H_{A_2} = 0.4$ kOe. However, demagnetization effects due to a plate-like shape of the FM domains would produce the same kind of anisotropy, and, therefore, a distinction between these two sources of anisotropy is not possible [22].

These FMR signals were observed in the PM regime above T_C in single crystals with Sr concentrations $x =$

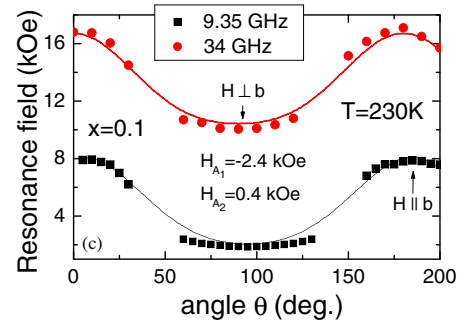


FIG. 2 (color online). Orientation dependence of the resonance field of the FMR at 9.35 and 34 GHz for $x = 0.1$ at 230 K. Fitting curves were obtained by assuming an easy-plane ($\perp b$) anisotropy [22].

0.075, 0.1, 0.125, and 0.5. They all separate from the PM signal below 270 K, indicating a temperature scale T_G above T_C which is almost independent of x , and they all exhibit the same anisotropy as shown in Fig. 2. Remarkably, no such additional FMR signals could be identified above T_C for samples with $x > 0.175$, which already exhibit a FM metallic ground state. Moreover, for $x \leq 0.05$ no FMR was observed in the PM regime, suggesting the existence of a lower Sr concentration threshold x_c with $0.05 < x_c < 0.075$. The fact that the phenomenon is not observable outside this concentration range confirms the intrinsic nature of the FMR signals.

In Fig. 3, we show susceptibility data for a sample with $x = 0.1$ (upper panel) together with the T dependence of the resonance fields of both the FMR and the PM signal (lower panel). For a large applied magnetic field (1 kOe), the FM component is hidden in the PM contribution and a CW law is found throughout the PM regime, while in small magnetic fields (10 Oe), clear deviations from a CW behavior are observed below $T_G = 270$ K [Fig. 3(a)], in agreement with the evolution of the FMR intensity (lower inset in Fig. 1). This temperature agrees very well with the extrapolation of the FMR shift with respect to $g = 2$ using a mean-field saturation behavior $\propto (1 - T/T_G)^{1/2}$ [Fig. 3(b)]. Plotting the obtained temperatures $T_G(x)$ within the T - x phase diagram of LSMO [Fig. 4(c)] [21,23,24], we obtain a novel phase regime within the PM region with an almost constant upper temperature boundary $T_G(x) \simeq T_C$ ($x \sim 0.16$).

Having identified the new phase regime in low doped LSMO, we will now discuss its interpretation in the context of quenched disorder as an enhanced GP becoming observable due to the competition of two ordering phases [6]. The source of disorder is the random substitution of La^{3+} by ions with different size and valence, such as Sr or Ca. The probability $p(x)$ for the existence of a FM bond increases with x , because the increasing number of Mn^{3+} - Mn^{4+} pairs enhances the double-exchange (DE) driven FM interaction. Because of the static Jahn-Teller (JT) distortion of the Mn^{3+} ions, the non-JT active Mn^{4+}

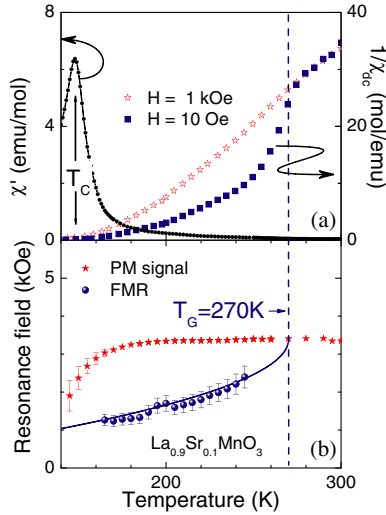


FIG. 3 (color online). T dependence of (a) the ac susceptibility ($H_{ac} = 1$ Oe, $f_{ac} = 10$ Hz) and the inverse dc susceptibility at 10 Oe and 1 kOe, and (b) the resonance fields of the FMR and the PM signal for $x = 0.1$. The solid line describes the FMR shift $\propto (1 - T/T_G)^{1/2}$. The external magnetic field was applied within the easy ac plane.

ions and the FM bonds can be regarded as fixed within the lattice (quenched disorder).

The lower bound T_G for the nonanalyticity of the magnetization is identified with the appearance of the FMR signals at $T \approx 270$ K. From the intersection of the T_G boundary with the magnetic ordering boundary, the regular ferromagnet corresponding to $p = 1$ is found to be at $x \sim 0.16$. In Bray's generalization of Griffiths' concept to FM systems with an arbitrary distribution of bond strengths, the Griffiths temperature scale T_G is no longer the critical temperature of the pure FM system with $p = 1$ but the maximal critical temperature among all configurations compatible with the static nature of disorder [25]. In our case, the static disorder is annealed above $x_{\max} \sim 0.16$ as a consequence of the transition from the JT distorted orthorhombic to the rhombohedral phase, i.e., as the random locations of the FM bonds begin to fluctuate concomitantly with the fluctuating lattice distortions. Consequently, the Griffiths phenomenon disappears for $x > 0.16$. The importance of this orthorhombic to rhombohedral transition has recently been reported to be crucial for the appearance of signatures of correlated clusters above T_C [26].

The threshold regime $0.05 < x_c < 0.075$ derived from the existence of the FMR in our ESR spectra can be refined by the results of neutron-diffraction studies in a single crystal with $x = 0.07$. At this concentration, the system is mainly in the canted AFM state, but an estimated 10% of the crystal volume is in a FM state [27]. In contrast, for $x = 0.06$ no such features were found [28], narrowing the percolation threshold regime down to $0.06 < x_c < 0.075$. To estimate x_c for FM bonds via DE, we start with a sc lattice of Mn^{3+} ions with lattice constant a . Assuming that

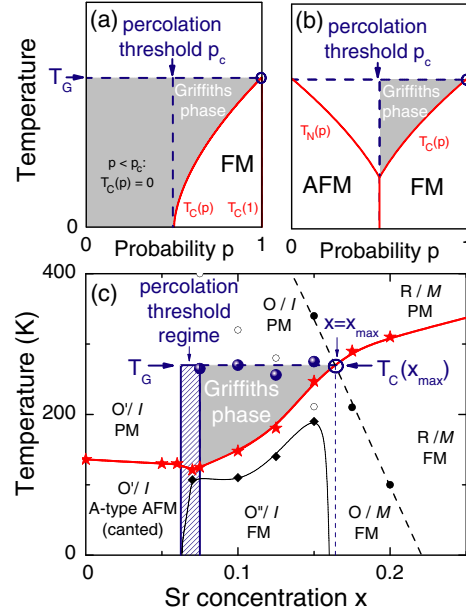


FIG. 4 (color online). (a) T - p diagram for the dilute FM Ising model [5]. (b) Conjectured schematic T - p diagram of the GP arising in a $\pm J$ random Ising model due to the competition of FM/AFM clusters; (c) observed Griffiths-phase boundaries within the established T - x phase diagram of LSMO [21]. The intersection (open circle) of T_G (spheres) with the magnetic boundary T_C (stars) coincides with the phase transition from the orthorhombic (O) to rhombohedral (R) structure ($I =$ insulator, $M =$ metal). Data for $x = 0.06$ and 0.07 were taken from Refs. [27,28], respectively. Lines are drawn to guide the eye.

upon doping only linear Mn^{3+} - Mn^{4+} - Mn^{3+} clusters form a sc lattice (percolation threshold $p_c^{sc} = 0.3116$ [29]) with lattice constant $2a$, only 1/8 of the sites are occupied by Mn^{4+} ions, resulting in a lower bound $x_c^l = p_c^{sc}/8 \approx 0.04$. Similarly, the staggered-square cluster with two Mn^{4+} and two Mn^{3+} ions results in a fcc lattice ($p_c^{fcc} = 0.198$ [29]), where half of the sites are occupied by Mn^{4+} ions. Thus, we derive an upper bound $x_c^u = p_c^{fcc}/2 \approx 0.1$ and obtain $0.04 < x_c < 0.1$ in good agreement with experiment.

Keeping in mind that the disorder in LSMO is quenched within the JT-distorted structure, it becomes clear that the disorder must be of a correlated nature as assumed in the argument above. In the case of theoretical models which include correlated disorder, it was found that Griffiths effects are enhanced [11,13]. Additionally, the existence of AFM bonds in the system and the resulting two-phase competition have to be considered and, indeed, Burgy *et al.* [4,6] argue on theoretical grounds that the existence of competing phases stabilizes and enhances FM Griffiths-like effects. In the presence of AFM clusters, the GP should be confined to a restricted region of the T - p phase diagram as depicted in Fig. 4(b).

Correlated disorder was considered by Vojta, who studied the Griffiths phenomenon in a 3D Ising FM with

planar defects [13]. As expected, the correlated disorder simply makes the large, rare clusters responsible for the Griffiths singularities much more likely to occur, thus strengthening considerably the Griffiths phenomenon. We believe this correlated-disorder enhancement, together with the two-phase AFM/FM competition, to be responsible for the observability of the otherwise weak Griffiths singularities. The critical behavior at the magnetic ordering temperature in LSMO has been studied in detail by Oleaga *et al.* through thermal diffusivity measurements [30]. These authors can describe the PM-AFM phase transition for $x < 0.1$ by a 3D-Heisenberg-type behavior, while for the PM-FM transition for $x > 0.28$ a 3D-Ising model is suggested. In the concentration range $0.1 < x < 0.28$, no universal behavior was found in agreement with theoretical expectations [13].

The existence of such a novel phase regime characterized by the FMR features is not restricted to weakly doped LSMO but rather represents a generic feature of manganite systems where the structural distortions are sufficiently strong to allow for the bond disorder to be completely quenched: The coexistence of PM and FMR signals above T_C has already been reported for some samples of the layered $\text{La}_{2-2x}\text{Sr}_{1+2x}\text{Mn}_2\text{O}_7$ manganites [31,32], but a complete ESR mapping of this system has not yet been performed. At the temperature scale where the FMR signal appears in these compounds, the onset of correlated polaronic behavior has been reported by neutron-diffraction studies [26,33]. Recently, Chapman *et al.* reported similar features for a series of polycrystalline $\text{Ln}_{0.7}\text{M}_{0.3}\text{MnO}_3$ samples with $\text{Ln} = \text{La, Pr, Nd, Sm}$ and $M = \text{Ca, Sr, Ba}$ [34], increasing the number of systems where Griffiths-phase regimes can be expected.

The observed value of $T_G = 270$ K is naturally explained through the influence of the structural transition which anneals the disorder distribution at $x \approx 0.16$. For $x > 0.16$, the time scale of the disorder fluctuations is no longer much greater than the dynamical scale of the order-parameter fluctuations, and the Griffiths singularities disappear. In this regime (rhombohedral phase), a description based on magnetic polarons coupled to the lattice distortions is suitable. For $x < 0.16$, the lattice distortions are essentially frozen, providing the fixed background of FM bonds in the PM insulating state. This quenched nature of the FM bond configuration agrees with the fact that no significant changes in the resistivity have been observed at T_G in LSMO [35]. This picture is valid above the transition to the FM insulator, below which the orbital degrees of freedom come into play.

In conclusion, we have experimentally identified, to the best of our knowledge, for the first time an entire Griffiths phase in the T - x phase diagram of LSMO by means of ESR and susceptibility measurements. This phase regime arises as a result of the strong quenching of the randomly diluted locations of the FM bonds in the cooperatively JT-distorted

structure and can be expected to be a generic feature in manganites. The enhanced visibility of these effects in manganites and the characteristic ESR features challenge further theoretical studies on the base of models which incorporate both FM/AFM phase competition and quenched disorder.

We thank M.V. Eremin, K.-H. Höck, T. Kopp, L. Svistov, D. Zakharov, and K. Ziegler for fruitful discussions. This work was supported by the BMBF via Contract No. VDI/EKM 13N6917 and partly by the DFG via SFB 484 (Augsburg). Support from MUIR through a COFIN-2003 project (G.J.) and from BRHE/REC007 (R.M.E.) is also acknowledged.

-
- [1] D. Akahoshi *et al.*, Phys. Rev. Lett. **90**, 177203 (2003).
 - [2] T. Nakajima *et al.*, J. Phys. Soc. Jpn. **73**, 2283 (2004).
 - [3] E. Dagotto *et al.*, Phys. Rep. **344**, 1 (2001).
 - [4] J. Burgy *et al.*, Phys. Rev. Lett. **92**, 097202 (2004).
 - [5] R.B. Griffiths, Phys. Rev. Lett. **23**, 17 (1969).
 - [6] J. Burgy *et al.*, Phys. Rev. Lett. **87**, 277202 (2001).
 - [7] E. Dagotto, New J. Phys. **7**, 67 (2005).
 - [8] M.B. Salamon *et al.*, Phys. Rev. Lett. **88**, 197203 (2002).
 - [9] J.M. de Teresa *et al.*, Nature (London) **386**, 256 (1997).
 - [10] A.J. Bray, Phys. Rev. Lett. **59**, 586 (1987).
 - [11] B. McCoy and T.T. Wu, Phys. Rev. B **176**, 631 (1968); **188**, 982 (1969).
 - [12] R. Shankar and G. Murthy, Phys. Rev. B **36**, 536 (1987).
 - [13] T. Vojta, J. Phys. A **36**, 10921 (2003).
 - [14] A.H. Castro-Neto *et al.*, Phys. Rev. Lett. **81**, 3531 (1998).
 - [15] V.M. Galitski *et al.*, Phys. Rev. Lett. **92**, 177203 (2004).
 - [16] A. Urushibara *et al.*, Phys. Rev. B **51**, 14 103 (1995).
 - [17] V.A. Ivanshin *et al.*, Phys. Rev. B **61**, 6213 (2000).
 - [18] J. Deisenhofer *et al.*, Phys. Rev. B **68**, 214427 (2003).
 - [19] J. Deisenhofer *et al.*, Phys. Rev. B **65**, 104440 (2002).
 - [20] B.I. Kochelaev *et al.*, Mod. Phys. Lett. B **17**, 459 (2003).
 - [21] M. Paraskevopoulos *et al.*, J. Phys. Condens. Matter **12**, 3993 (2000).
 - [22] A.G. Gurevich and G.A. Melkov, *Magnetization Oscillations and Waves* (CRC Press, Boca Raton, FL, 1996).
 - [23] B. Dabrowski *et al.*, Phys. Rev. B **60**, 7006 (1999).
 - [24] R. Klingeler *et al.*, Phys. Rev. B **65**, 174404 (2002).
 - [25] A.J. Bray and G.J. Rodgers, J. Phys. C **21**, L243 (1988).
 - [26] V. Kiryukhin, New J. Phys. **6**, 155 (2004).
 - [27] S.F. Dubunin *et al.*, Phys. Solid State **45**, 2297 (2003).
 - [28] M. Hennion *et al.*, Phys. Rev. Lett. **81**, 1957 (1998).
 - [29] D. Stauffer and A. Aharony, *Introduction to Percolation Theory* (Taylor & Francis, London, 1992).
 - [30] A. Oleaga *et al.*, Phys. Rev. B **70**, 184402 (2004).
 - [31] O. Chauvet *et al.*, Phys. Rev. Lett. **81**, 1102 (1998).
 - [32] F. Simon *et al.*, Phys. Rev. B **67**, 224433 (2003).
 - [33] D.N. Argyriou *et al.*, Phys. Rev. Lett. **89**, 036401 (2002).
 - [34] J.P. Chapman *et al.*, Dalton Trans. **19**, 3026 (2004).
 - [35] E.V. Mostovshchikova *et al.*, Phys. Rev. B **70**, 012406 (2004).